ORIGINAL PAPER

Mathematical Modeling and Simulation of Microwave Thawing of Large Solid Foods Under Different Operating Conditions

Laura Analía Campañone · Noemi E. Zaritzky

Abstract Microwaves require shorter times to increase food-stuffs temperature when compared to conventional heating methods. However, there are some problems associated to temperature distribution within the products, owing to the preferential absorption of electromagnetic energy by liquid water, caused by differences between its dielectric properties and those of ice ("runaway"). To analyze the behavior of food microwave thawing, a mathematical three-dimensional (3D) model was developed by solving the unsteady-state heat and mass transfer differential equations; this model can be applied to large systems for which Lambert's law is valid. Thermal, mass transport, and electromagnetic properties varying with temperature were used. The numerical solution was developed using an implicit Crank–Nicolson finite difference method using the classical formulation for one-dimensional (1D) systems and the alternating direction method in two and three dimensions. The model was validated using experimental data from the literature for 1D and two-dimensional conditions and with experiments performed in our laboratory for 3D heat transfer using frozen meat. It was applied to predict temperature and water concentration profiles under different thawing conditions in meat products and to simulate the effect of a fat layer located at the surface of the meat piece on temperature profiles. For different product sizes in rectangular geometry, numerical simulations demonstrated that microwave thawing times were significantly lower in comparison to conventional thawing methods. To prevent overheating during thawing, the combination of continuous microwave power with simultaneous application of air convection and the application of microwave power cycles, using refrigerated air convection with controlled surface temperature, were analyzed.

Keywords Microwaves · Thawing · Mathematical modeling

L. A. Campañone · N. E. Zaritzky (✉)
Centro de Investigación y Desarrollo en Criotecnología de
Alimentos (CIDCA), UNLP-CONICET La Plata,
47 y 116 (B1900AJJ),
La Plata, Buenos Aires, Argentina
e-mail: zaritzky@ing.unlp.edu.ar

L. A. Campañone · N. E. Zaritzky
Departamento de Ingeniería Química, Facultad Ingeniería,
Universidad Nacional de La Plata,
La Plata, Argentina

Introduction

Microwave heating is an attractive alternative over food conventional heating methods because electromagnetic wave that penetrates the product surface is converted into thermal energy within the material. This technology is used in many industrial and household applications (Cha-um et al. 2009). It has been used in the food industry for baking, drying, pasteurization, sterilization, blanching, thawing, etc. (Burfoot et al. 1996; Lin et al. 1998; Datta and Anantheswaran 2001; Ahmed and Ramaswamy 2007; Jeong et al. 2007; Turabi et al. 2008; Sakiyan et al. 2009). One of the major problems associated with microwave heating is the nonuniform temperature distribution; this subject has been studied and mathematically modeled by several researchers in solid and liquid systems (Ayappa 1997; Oliveira and Franca 2002; Campañone and Zaritzky 2005; Gunasekaran and Yang 2007; Vadivambal and Jayas 2009).

Freezing is an efficient and widespread method for food preservation. The industry keeps raw materials frozen and the thawing procedures used are often slow and exposed to risks of microbial growth, product spoilage, and excessive drip production. The use of microwaves during thawing speeds up the process owing to its inherent capacity to

generate energy inside the product by the interaction of this radiation with water molecules. Even a food with a low thermal conductivity can be rapidly thawed using microwaves, which is not possible using conventional methods. However, problems do exist with microwave thawing, mainly related to some uneven temperature distributions inside the food. This occurs by preferential absorption of electromagnetic energy in liquid water compared to ice caused by differences in dielectric properties ("runaway"). Then, during microwave thawing, ice can persist in some zones while liquid water evaporates in other regions; this fact has been a determining factor for the industrial application of microwave technology (Taoukis et al. 1987).

To determine temperature distribution inside the foods, several authors have treated microwave thawing from a mathematical point of view. Modeling must solve the coupled distribution of temperature and moisture considering the absorption of electromagnetic energy within the product. To evaluate the electromagnetic field distribution, Maxwell equations, which govern the propagation of radiation in a dielectric medium, were used by several authors to model microwave thawing (Pangrle et al. 1991; Lee and Marchant 1999; Basak and Ayappa 2002).

Another way to model the microwave thawing process is to use Lambert's law, which considers an exponential energy decrease inside the product (Taoukis et al. 1987; Tong and Lund 1993; Zeng and Faghri 1994; Lin et al. 1995; Chamchong and Datta 1999; Taher and Farid 2001; Liu et al. 2005).

Lambert's law equation can be applied rigorously in products whose size is larger than a critical value; its use is subject of controversy (Curet et al. 2007). The critical value depends on the geometry and size of the product and also on its dielectric properties. Ayappa et al. (1991) and Ayappa (1997) reported an equation to calculate the critical size of slabs under microwave heating process. These authors established that Maxwell and Lambert predictions differed in 1% when slab thickness is higher than three times the microwave penetration. Oliveira and Franca (2002) reported a more restrictive equation for heated cylinders than that obtained by Ayappa et al. (1991), establishing that Lambert's law can be applied when the diameter is seven times higher than microwave penetration. Liu et al. (2005) compared these laws when modeling the microwave thawing of tuna slabs and demonstrated that both Maxwell and Lambert equations can describe temperature profiles successfully. However, certain aspects are important to be analyzed, such as the three-dimensional (3D) modeling of the simultaneous heat and mass transfer of microwave thawing using Lambert's law and its application to homogeneous and heterogeneous food systems, considering the different thermal and electromagnetic properties of each layer.

Related to these considerations the objectives of the present work were:

1. To develop a 3D model in order to calculate temperature and moisture distributions inside large blocks of frozen meat products submitted to microwave thawing.
2. To solve the coupled mass and energy balances considering (a) thermal, mass transport, and electromagnetic properties varying with temperature and (b) electromagnetic energy absorption given by Lambert's law that can be applied to large systems as a valid simplification.
3. To validate the numerical solution with experimental data from the literature for one-dimensional (1D) and two-dimensional (2D) conditions and with experiments performed in our laboratory for 3D heat transfer.
4. To apply the validated model to simulate (a) the effect of a fat layer located at the surface of the meat piece on temperature profiles; (b) the influence of product size on microwave thawing times in comparison with conventional thawing; (c) the combination of continuous microwave power with simultaneous application of air convection in order to attain increasing uniformity on the temperature profiles; and (d) the application of microwave power cycles and refrigerated air convection with controlled surface temperature to prevent overheating during thawing.

Mathematical Modeling

To predict temperature and moisture profiles during product thawing, the proposed mathematical model was developed with the following assumptions:

1- 3D heat and mass transfer with rectangular geometry is considered.
2- Initial temperature and concentration profiles are uniform in the products.
3- Lambert's law is applied to describe microwave spatial distribution inside large food pieces.
4- The thermal, transport, and dielectric properties are temperature-dependent.
5- No volume changes are considered during thawing.
6- Boundary conditions are of convective type.

To describe heat transfer, the equations were similar to those in conventional thawing with an additional term of internal heat generation to account for the microwave energy (Ayappa 1997). Therefore, the microscopic energy balance is as follows:

$$\rho \mathrm{Cap} \frac{\partial T}{\partial t} = \nabla(k\nabla T) + Q \tag{1}$$

where T is the temperature (in degrees Celsius), t is the time (in seconds), ρ is the density (in kilograms per cubic meter), Cap is the apparent specific heat (in Joules per kilogram per degrees Celsius), k is the thermal conductivity (in Watts per meter per Kelvin), and Q is the heat source per unit volume that is a function of position and temperature (in Watts per cubic meter).

The model uses an apparent specific heat (Sanz et al. 1987; Campañone 2001), which groups the sensible specific heat and the ice solidification enthalpy (L_f, in Joules per kilogram):

$$\text{Cap}_{(T < T_{if})} = \text{Cap}_{(T > T_{if})} - L_f Y_o \frac{\partial w}{\partial T} \tag{2}$$

where T_{if} is the initial melting point, Y_o is the water content, and w is the ice content (in kilograms of ice per kilogram of water). In terms of power (in Watts), Eq. 1 can be rewritten as:

$$V\rho\text{Cap}\frac{\partial T}{\partial t} = V(\nabla k \nabla T) + P \tag{3}$$

where V (in cubic meters) is the product volume and P (in Watts) is the power generated by microwave absorption that depends on the spatial coordinates and the dielectric properties of the foodstuff.

The model was developed in 3D considering a rectangular parallelepiped (dimensions: Lx, Ly, Lz); however, due to the symmetry, it was solved between the center and the surface in each direction.

To solve the microscopic energy balance, the following initial condition was considered:

$$t = 0 \quad T = T_{ini} \quad 0 \le x \le Lx/2, \quad 0 \le y \le Ly/2,$$
$$0 \le z \le Lz/2. \tag{4}$$

Boundary conditions were applied for the three Cartesian coordinates (x, y, z) in 3D formulation. Taking into account that similar expressions for the boundary conditions are valid for all the spatial directions, only expressions in the x coordinate are written:

$$x = 0 \quad -k\frac{\partial T}{\partial x} = 0 \quad t > 0 \tag{5}$$

$$x = Lx/2 \quad -k\frac{\partial T}{\partial x} = h(T - T_a) + \Delta H_{vap}\, k'_m \left(C_w - C_{equi}\right) \tag{6}$$

where T_{ini} (in degrees Celsius) is the initial temperature, h (in Watts per square meter per degrees Celsius) is the heat transfer coefficient, T_a (in degrees Celsius) is the air temperature, ΔH_{vap} (in Joules per kilogram) is the latent heat of vaporization, C_w is the product water concentration at the interface (in kilograms of water per cubic meter of

product), and C_{equi} the equilibrium water concentration from the sorption isotherm (in kilograms of water per cubic meter of product), and k'_m (in meters per second) is the mass transfer coefficient in the surrounding air, defined in terms of water vapor concentration in the product. Equation 6 represents the boundary condition at the border (food–air interface) in which surface evaporative heat losses during thawing were taken into account.

The model considers the analogy between heat and mass transfer to evaluate k'_m. The Chilton and Colburn J factors for heat and mass transfer $J_H = J_D \left(\frac{Nu}{Re\,Pr^{1/3}} = \frac{Sh}{Re\,Sc^{1/3}}\right)$ allowed to estimate k'_m from h values (Bird et al. 1976).

The symmetry condition at the center (Eq. 5) is valid in the cases in which heat transfer takes place in a sample placed in the center of the oven on a support made by a material transparent to microwave radiation, such as acrylic, that has a very low loss factor and all faces are exposed to the radiation. In the simulations of experiments in which the samples were placed directly on the floor of the microwave oven, the insulating condition was applied at the bottom surface.

The model was considered valid until the surface temperature reaches 100 °C and corresponds to a weak dehydration process formulation without changes in the sample porosity. This formulation differs from the behavior that occurs at higher temperatures in which water vaporization and vapor diffusion are produced inside the whole system.

To describe the moisture profile during product thawing, the microscopic mass balance was proposed assuming mass transport according to Fick's law with a temperature-dependent diffusion coefficient D_w (in square meters per second). Then, the mass transport formulation in 3D is as follows:

$$\frac{\partial C_w}{\partial t} = \nabla(D_w \nabla C_w). \tag{7}$$

To solve the mass balance, the following initial and boundary conditions were considered:

$$t = 0 \quad C_w = C_{w,ini} \quad 0 \le x \le Lx/2,$$
$$0 \le y \le Ly/2, \quad 0 \le z \le Lz/2. \tag{8}$$

Similarly to heat transfer formulation, only boundary conditions for the x coordinate are shown:

$$x = 0 \quad \frac{\partial C_w}{\partial x} = 0 \quad t > 0 \tag{9}$$

$$x = Lx/2 \quad -D_w\frac{\partial C_w}{\partial x} = k'_m\left(C_w - C_{equi}\right) \quad t > 0 \tag{10}$$

where D_w is the diffusion coefficient of the liquid water.

The power absorbed by materials during microwave thawing at different positions of the sample is given by

Lambert's law where heat generation is a function of temperature at a given position (Lin et al. 1995). A generic formulation of Lambert's law is as follows:

$$P = P_o e^{(-2\alpha(L-s))} \tag{11}$$

where P is the absorbed power, P_o (in Watts) is the microwave power generation at the surface of the product, L generically represents the half thickness (Lx/2, Ly/2, or Lz/2) in a given direction s (x, y, or z), and α is the attenuation factor (1/m). The value of α depends on frequency and temperature through the dielectric constant ε' (dimensionless) and the loss factor ε'' (dimensionless), being tan δ the loss tangent or dissipation factor:

$$\alpha = \frac{2\pi}{\lambda} \sqrt{\frac{\varepsilon'\left[(1+\tan^2\delta)^{1/2}-1\right]}{2}}. \tag{12}$$

Lambert's law assumes that the spatial distribution of absorption is an exponential decay and is strictly valid for semi-infinite media or for large pieces of foodstuffs in which microwave penetration is lower than L. Equation 11 was applied in each direction of the 3D formulation.

Ice and frozen foods exhibit a very low dielectric loss factors and large penetration values in comparison with unfrozen products. The penetration depth determines the amount of heat generated at a particular location considering the exponential decay of power.

Penetration depth is defined as the distance at which the microwave power is reduced to $1/e$ (1/2.718337=37%) of its surface value and is related to the reciprocal of α. At 2,450 MHz for liquid water at 25 °C, ε'=78, ε''=12.48, and tan δ=0.16. In the case of ice at −12 °C, ε'=3.2, ε''= 0.0029, tan δ=0.00091 (Hui 2006).

The microwave energy was able to permeate more deeply inside a sample in the frozen state, and surface heating became stronger after thawing (Ayappa 1997).

During the thawing process, a moving front between frozen and unfrozen zones was considered; the position of the front in each direction (x, y, z) as a function of time is given by λ. The presence of these two phases, with their corresponding dielectric properties, leads to different absorption capacities of the microwave radiation that must be calculated.

In order to show, in a simplified way, the calculation of the actual absorbed power (P_{abs}), the equations shown below were developed for a 1D domain (x coordinate). The schematic representation of 1D half thickness slab, indicating the position of the thawing front λ is observed in Fig. 1.

To calculate the actual absorbed power (P_{abs}, in Watts), the following expression has to be solved:

$$P_{abs} = \int_0^\lambda \left.\frac{dP}{dx}\right|_f A dx + \int_\lambda^L \left.\frac{dP}{dx}\right|_{th} A dx. \tag{13}$$
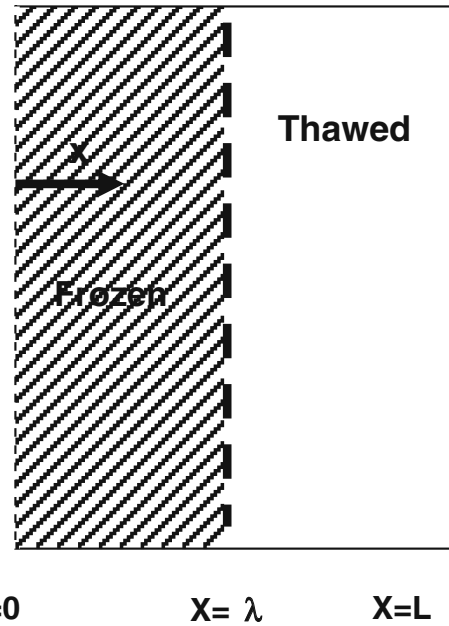

Fig. 1 Coordinates of the heat and mass transfer model and the position of the moving thawing front (λ)

The derivatives with respect to the x coordinate of the power values corresponding to the frozen (f) and thawed (th) zones are given by the following expressions:

$$\left.\frac{dP}{dx}\right|_f = P_o^* 2\alpha_f e^{-2a_{th}(L-\lambda)} e^{-2a_f(\lambda-x)}, \tag{14}$$

$$\left.\frac{dP}{dx}\right|_{th} = P_o^* 2\alpha_{th} e^{-2\alpha_{th}(L-x)} \tag{15}$$

where P_o^* is the maximum power at $x=L$ (in Watts per square meter).

By replacing Eqs. 14 and 15 in Eq. 13 and integrating between the limits of frozen (f) and thawed (th) zones, the following expression was obtained:

$$P_{abs} = P_o^* A\left[1 - e^{-2\alpha_{th}(L-\lambda)} - e^{-2\alpha_{th}(L-\lambda)}\left(1 - e^{-2\alpha_f\lambda}\right)\right] = P_o f \tag{16}$$

where $P_o = P_o^* A$ and f is the energy fraction absorbed by the foodstuff when it is partially thawed and can be calculated as a function of the position of the thawing front.

This procedure explained for the x coordinate that was repeated for the other coordinates y and z.

Modeling of a Slab Containing a Surface Fat Layer

One of the aims of the present work is to analyze temperature profiles and to predict thawing times in meat containing surface fat layers. Energy balances were solved in the product (meat) and in the fat layer using the corresponding temperature-dependent properties. For the fat layer, as in the

case of lean meat, Cp is the apparent specific heat which accounts for the change of phase during thawing; besides, the melting of the fat in the range of temperatures between 13.8 and 47.9 °C was also considered.

For the meat containing a fat layer, the following conditions were proposed: initial condition (Eq. 4) in the whole product, symmetry condition (Eq. 5) at the center, and convective condition (Eq. 6) at the fat–air interface without water vaporization.

The following boundary condition at the meat–fat interface was considered:

$$-k \frac{\partial T}{\partial x} = -k_{\text{fat}} \frac{\partial T}{\partial x} \quad t > 0 \tag{17}$$

The fat layer has low dielectric properties compared with water; however, induced polarization occurs in fats and oils causing molecular friction to convert electromagnetic energy to thermal energy. Moreover, the low specific heat of fat thus requires less thermal energy for a given amount of fat to increase in temperature. It also contributes to an increase in the food temperature during the fat melting process.

To calculate P_{abs}, the presence of a fat layer was considered as follows:

$$P = P_{\text{o}}^{*} 2\alpha_{\text{fat}} e^{\left(-2\alpha_{\text{fat}}(L+\text{FT}-x)\right)} \tag{18}$$

where FT is the thickness of the fat layer.

According to the previously described procedure, the obtained equation to calculate P_{abs} for the complete system: meat–fat is as follows:

$$P_{\text{abs}} = P_{\text{o}}^{*} A \left[1 - e^{-2\alpha_{\text{fat}}\text{FT}} + e^{-2\alpha_{\text{fat}}\text{FT}} \left(1 - e^{-2\alpha_{\text{th}}(L-\lambda)} - e^{-2\alpha_{\text{th}}(L-\lambda)} \left(1 - e^{-2\alpha_{\text{f}}\lambda} \right) \right) \right] = P_{\text{o}} f. \tag{19}$$

The expression corresponding to the power absorbed by the meat (adjacent to the fat layer):

$$P_{\text{abs, meat}} = P_{\text{o}}^{*} A e^{-2\alpha_{\text{fat}}\text{FT}} \left[1 - e^{-2\alpha_{\text{th}}(L-\lambda)} - e^{-2\alpha_{\text{th}}(L-\lambda)} \left(1 - e^{-2\alpha_{\text{f}}\lambda} \right) \right] = P_{\text{o}}' f' \tag{20}$$

where P_{o}' is the absorbed power at the fat–meat interface.

According to Eqs. 19 and 20, P_{abs} and $P_{\text{abs, meat}}$ are lower than the maximum value P_{o}^{*} (at the air–food interface) because f and f' are factors lower than 1.

Applications of the Mathematical Model

One of the most effective methods to minimize nonuniform temperature profiles and overheating in microwaves has been to cycle microwave power. Such cycling is generally done as a simple on–off operation; turning the oven on at full power during a fraction of time and turning it off during the rest of the cycle. The fraction of time the microwaves are off allows the nonuniform temperature profiles to equilibrate. The model was run in order to analyze the effect of power cycling on thawing times and temperature profiles and to study the effect of air convection (combined with microwaves) on thawing times and weight losses.

Materials and Methods

Numerical Solution

Energy and mass balances are coupled with each other, and form, together with their boundary conditions, a system of nonlinear differential equations. An implicit Crank–Nicolson finite difference scheme was used to solve the system numerically; the classical formulation was used in 1D heat and mass transfer (Campañone 2001). For 2D and 3D heat and mass transfer, an alternating direction method was employed (Cleland and Earle 1979; Cleland and Cleland 1991). In all cases, the selected Crank–Nicolson finite difference scheme is an inconditional stable method. A complete description of the numerical method was presented in Campañone and Zaritzky (2005). The solution of the equations system was programmed in Fortran 90 to calculate temperature and moisture contents.

From these moisture profiles, weight losses (WL; in kilogram of water per kilogram of sample) during thawing were predicted using the following equation:

$$\text{WL} = \frac{\int_{0}^{t} k_{\text{m}}' A \left(C_{\text{w}} - C_{\text{equi}} \right) \mathrm{d}t}{\rho V} \tag{21}$$

When analyzing the effect of power on–off cycles on temperature profiles, nonuniformity of temperature profiles (NU) was calculated from the following expression:

$$\text{NU} = \sqrt{\frac{\sum_{i=1}^{N_n} \left(T_i - \overline{T} \right)^2}{N_n}} \tag{22}$$

where T_i is the temperatures at the nodes, T is the average sample temperature, and N_n is the number of nodes in the domain.

The numerical model was fed with experimental data obtained from independent experiments, i.e., absorbed power, and from the literature (thermophysical, transport, and dielectric properties). Experimental data from the literature (1D and 2D systems) and experiments representing 3D transfer conditions (carried out in our laboratory) were used to validate the model.

Functions that represent apparent specific heat, thermal conductivity, density, water diffusivity, and dielectric properties of frozen and thawed products (meat and tylose) and for meat–fat used in the numerical model are shown in Table 1.

Determination of the Electromagnetic Power Absorbed by a Water Sample

The electromagnetic power absorbed by a water sample (P_o) was determined by experimental measurements using different water volumes.

However, the absorbed power at the surface depends on the characteristics of the product reaching the highest values for thawed products. Then, the values of P_o determined for water were corrected for the case of unfrozen, partially frozen, or totally frozen product using the f factor.

The electromagnetic power absorbed by a water sample was assessed by means of a calorimetric method (Lin et al. 1995). The technique consists of calculating the power absorbed by different volumes of water on heating under the same operating conditions (position, power, and container size) as those used in the experiments with meat products.

Absorbed power was calculated through the following expression:

$$P_o = m_w \, Cp_w \frac{\Delta T}{\Delta t} \tag{23}$$

where m_w is the mass of liquid water (in kilograms), Cp_w is the specific heat of the water, ΔT is the increment of the temperature, and Δt is the heating time.

A polynomial model was proposed to relate power P_o (in Watts) with water content of the sample; the Systat 10 Statistical software (SYSTAT, Evanston, IL, USA, 2001) was used to estimate model parameters and calculate its deviation.

Validation of the Numerical Model

To validate the numerical method in 3D, microwave thawing experiments were carried out in duplicated samples. In frozen foods, microwave penetration depth at −20 °C is higher than 10 cm; however, when the thawing process begins, this value decreases significantly due to the change in the dielectric properties. Different authors (Chamchong and Datta 1999;

Table 1 Physical, transport and dielectric properties used in the mathematical model

Properties	Frozen meat ($T<-1.1$°C)	Thawed meat ($T>-1.1$°C)	Tylose	Frozen beef fat ($T<-1.1$°C)	Thawed beef fat ($T>-1.1$°C)
Density (kg/m³)	$\dfrac{1053}{0.98+0.11Y_o+0.26\left(1-\frac{Y_o}{T}\right)}^{a}$	$1{,}053^{a}$	940^{a}	965^{c}	$965-1.45T^{c},\ T<30$ °C $935-0.43T^{c},\ T>30$ °C
Thermal conductivity (W/(m °C))	$0.378+1.376Y_o+0.93/T^{a}$	$0.087+0.501Y_o+5.052\ 10^{-4}Y_oT^{a}$	1.65^{a}	$0.874-0.673e^{(0.0039T)c}$	$0.23+6.7\times10^{-3}T^{c},\ T<30$ °C $0.18-2.2\times10^{-4}T^{c},\ T>30$ °C
Specific heat (J/(kg °C))	$3{,}874-2{,}534Y_o+9.03\times10^{5}(1-Y_o)/T^{2a}$	$1{,}448(1-Y_o)+4{,}187Y_o{}^{a}$	$1{,}418.4^{a}$	$10^{3}\left(1.84+7\times10^{-3}T+\dfrac{2.24}{1+8.93\times10^{-3}(T-13.8)^{2}}+\dfrac{4.28}{1+2.34\times10^{-2}(T-47.85)^{2}}\right)^{c}$	
Attenuation factor (1/m)	$49.9+6.17+0.30T^{2}+0.005T^{3b}$	$50.52-0.157+0.0025T^{2}+6\times10^{-7}T^{3b}$	7.8^{e}	2^{d}	2.3^{d}
Water diffusion coefficient (m²/s)	10^{-12a}	$2\times10^{-12}T-1\times10^{-12a}$	–	–	

[a] Campañone (2001)

[b] Regression of experimental data of minced beef with of 20% fat content by Gunasekaran (2002)

[c] Houška (1997)

[d] From calculations with dielectric properties presented in Pace et al. (1968)

[e] Chamchong and Datta (1999)

Taher and Farid 2001) carried out experiments using samples smaller than 10 cm thickness. Samples of ground beef shaped as cubes (6 cm size) placed in glass containers, a material transparent to radiation, were used and they were frozen in a freezer at −20 °C for 24 h. Another set of samples was kept at −6 °C in a cold store. To simulate food thawing under typical conditions, experiments were conducted in a microwave oven (BGH model 17950, Argentina) with a maximum power of 1,000 W, operating at a frequency of 2,450 MHz. During the experiments, the samples were located at the center of the microwave oven, placed on an acrylic support on a rotating turntable. The rotation of the turntable allows a better uniformity of the electromagnetic field around the sample surface (Tong and Lund 1993; Geedipalli et al. 2007). The turntable rotated at a rate of one turn every 12 s. Previous to the freezing process, a small-diameter (2 mm) plastic tube was inserted from the external surface towards the center of the sample.This tube was transparent to microwave radiation and allowed to put immediately the thermocouple inside the tube each 12 s (one turn of the rotating plate) during the microwave thawing process after turning off the equipment.

Sample temperatures were measured before and after heating using type T thermocouples connected to the Keithley KDAC Series 500 (Orlando FL, USA) acquisition equipment interfaced to a personal computer.

Statistical Analysis

The average relative errors of the predicted thawing times (time required to reach 0 °C in the center of the sample) with respect to the experimental values were determined as follows:

$$Er\% = \frac{\sum_{j=1}^{N} \left| \frac{\left(t\,\exp_j - t\,\mathrm{pred}_j\right)}{t\,\exp_j} \right|}{N} \times 100. \qquad (24)$$

Results and Discussion

Validation of the Mathematical Model with Data from Literature

The mathematical model was validated by comparison of the predicted values with experimental thawing temperatures obtained from the literature for one and two dimensions heat transfer experiments. The computer code was run using a time interval of 0.1 s, being each direction of the spatial domain divided into 15 intervals. The model was fed with thermal and electromagnetic properties shown in Table 1 with the heat transfer coefficients reported in the literature and with the f factor calculated by using Eq. 16.

Figure 2 shows the calculated values of f for different positions of the thawing front (λ). It can be observed that, for
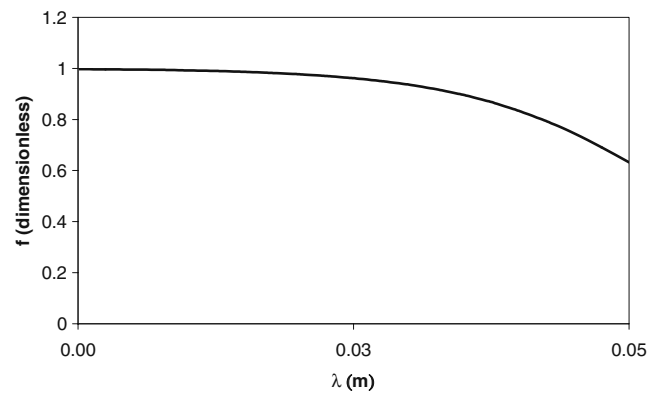

Fig. 2 Factor (f) that affects the absorbed microwave energy power as a function of the thawing front position in a meat slab irradiated from one side (Eq. 16). This factor depends on the relative amount of frozen and thawed fractions

frozen and partially frozen products, the absorbed power decreased by the f factor and for a totally thawed product ($\lambda = 0$), $f \to 1$. These results agree with the comments of Ni and Datta (2002). The authors reported that the surface flux in unfrozen foods is much lower than 1 in partially frozen foods due to much less absorption of microwave in frozen foods.

To validate the 1D transfer model, experimental data by Taher and Farid (2001) were utilized. These authors analyzed the thawing of ground beef shaped as a slab (4 cm thickness) and measured temperatures in different internal positions (0.4, 1, 1.6, 2.2, 2.8, and 3.4 cm). In Fig. 3a, the experimental data of Taher and Farid (2001) were plotted together with the numerical predictions of the present work. The average relative error between the model predictions and the experimental thawing times were lower than 12% similar to the error reported by the authors.

In 2D heat transfer, numerical predictions were validated using results reported by Chamchong and Datta (1999). In a tylose block (3% salt), these authors have measured temperatures at the center and 1 cm behind the surface during thawing. They reported initial and final temperatures for thawing using different power levels. Figure 3b shows the experimental values of Chamchong and Datta (1999) and those predicted by the present model using different power values (P_o). The agreement between numerical results and experimental data is satisfactory.

Validation of the Mathematical Model by Comparing the Numerical Solution with Three-Dimensional Heat Transfer Experiments

In 3D heat transfer, the model was validated by using experimental data obtained in our laboratory using ground beef cubes. The model used thermal properties of Campañone (2001) and electromagnetic properties of ground beef containing 20% fat mixed with the lean beef obtained from
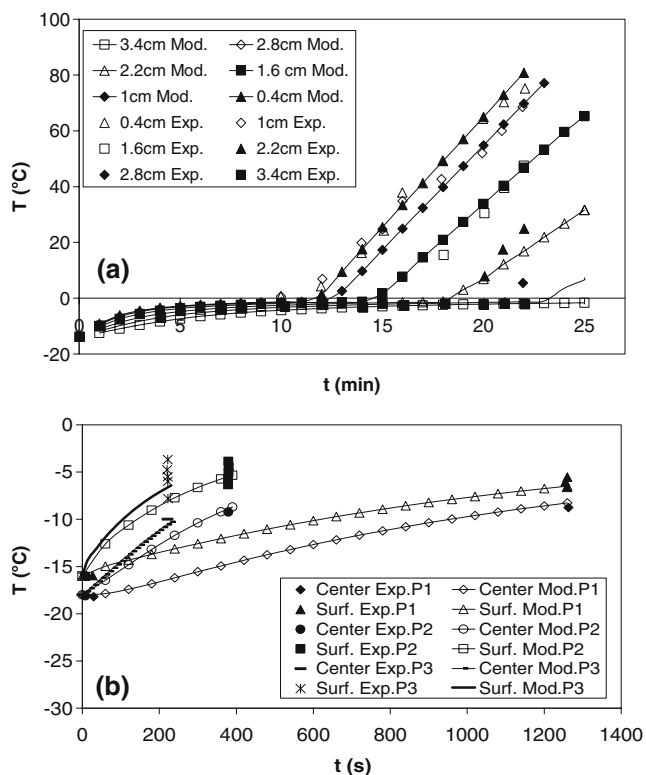
tal thawing times in the center and the corners was lower than 10%.

By analyzing the shape of the temperature profiles during thawing (Fig. 4a, b), it can be observed that the frozen region shows a flat profile until water melting begins. Then, the liquid fraction increases affecting the dielectric properties. The thawed product has a higher capacity to absorb radiation, while the frozen product is almost transparent (Mudgett 1982), then the temperature in the thawed region increases rapidly. The hot spot is located at the surface, as in conventional thawing, because the behavior predicted by Lambert's law assumes an exponential decay of energy absorption inside the product.

Assessment of the Mathematical Model

Once the model was validated, it was applied to predict temperature and water concentration profiles under different thawing conditions. The effects of product size and the presence of a fat layer on thawing times and temperature profiles with and without microwave treatment were simulated. Besides, the model was run to analyze the combined effect of air convection and microwave power cycles on thawing times.
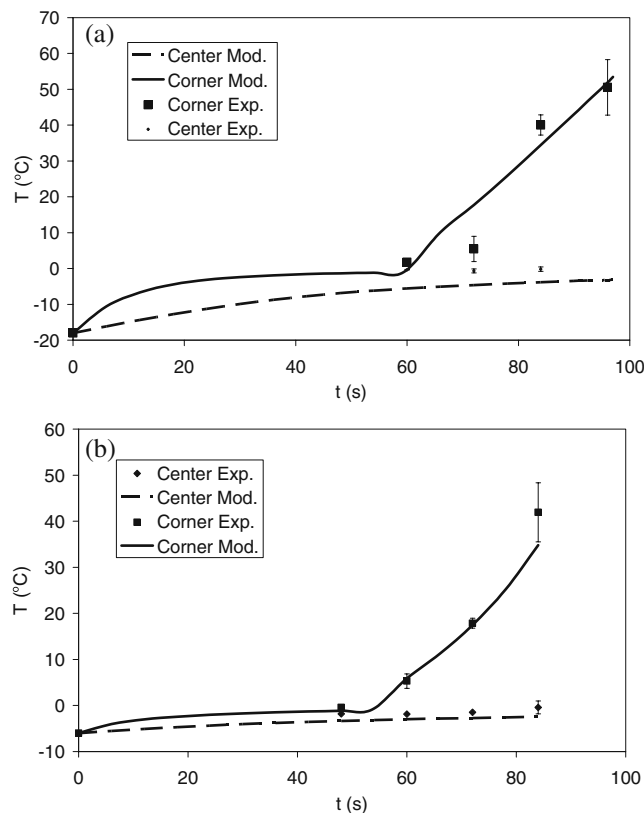
Fig. 3 **a** Model predictions (*continuous line + symbol*) for microwave thawing of ground beef and experimental data obtained by Taher and Farid (2001) in different internal positions (*symbols*), P_o=650 W. **b** Temperature profiles predicted by the numerical model and experimental results obtained in tylose bricks (*symbols*; Chamchong and Datta (1999)) for 2D heat transfer, for P_o=25,400 W/m^2, affected by different reducing percentages: P_1=2,450 W/m^2, P_2=12,700 W/m^2, P_3=17,780 W/m^2

Gunasekaran (2002; Table 1). A heat transfer coefficient h=5 W/(m^2 °C) was considered and the mass transfer coefficient in the surrounding air, defined in terms water vapor concentration in the solid, was obtained by analogy between heat and mass transfer ($k'_m = 4.081 \times 10^{-8}$ m/s).

Absorbed power was experimentally determined using Eq. 23 and the obtained regression equation is as follows:

$$P_o = 112.3 + 10.718W - 0.0845W^2 + 0.0002W^3,$$
$$50 \leq W(\text{gr}) \leq 200, r^2 = 0.945. \quad (25)$$

where W is the mass of water in grams

The power obtained through Eq. 25 was supplied as an input to solve the mathematical model, in which P_{abs} is a fraction of P_o.

Figure 4a, b shows the experimental values of temperature vs. time at the center and corners of the meat cubes plotted together with the corresponding numerical predictions. In these positions, the mathematical model satisfactorily predicts the temperature changes during microwave thawing. The average error between the predicted and the experimen-

Fig. 4 Temperature profiles predicted by the numerical model (present work) and experimental results (present work, *symbols*) obtained in ground beef cubes 6 cm side for 3D heat transfer **a** Tini=−18 °C, **b** Tini=−6 °C

Effect of Thawing Conditions on Temperature and Water Concentration Profiles

Figure 5 a, b shows the predicted temperature profiles in a minced beef cube (10 cm side, initial temperature=−18 °C, final temperature=0 °C (center) and air temperature=25 °C, relative humidity=75%, heat transfer coefficient h=5 W/
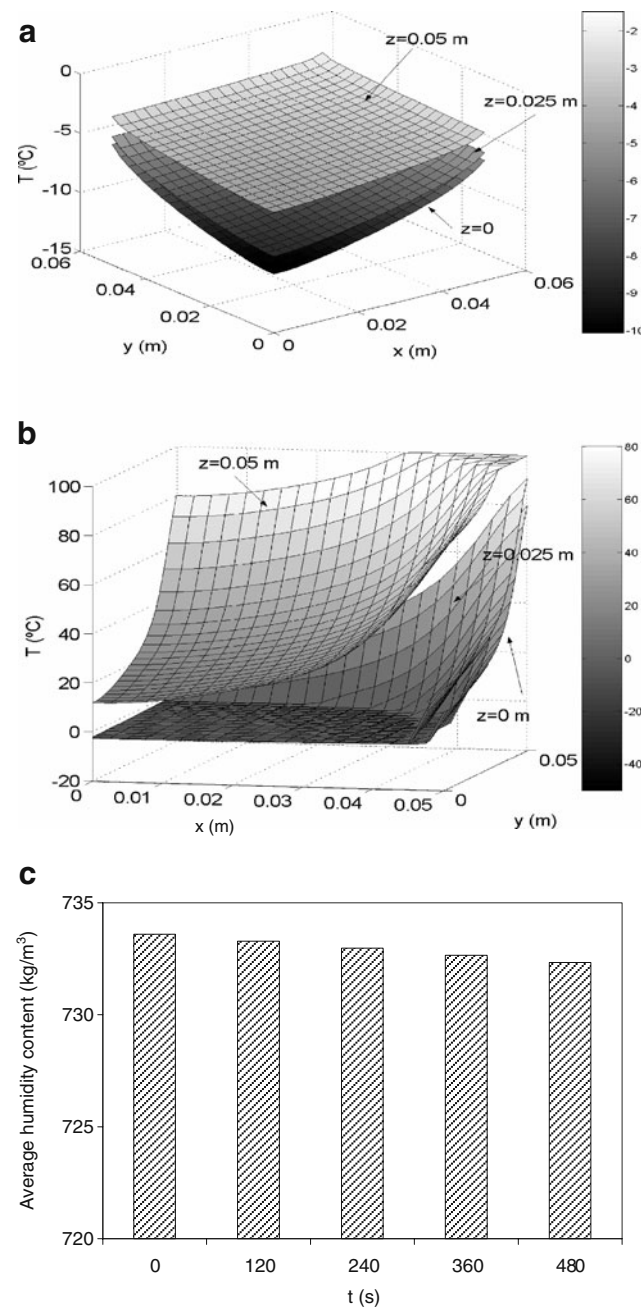
a

b

c

Fig. 5 Predicted temperature profiles in a minced meat cube **a** t= 120 s and **b** t=480 s; **c** changes in the average humidity content as a function of microwave thawing times for a minced meat. Cube side= 10 cm, initial temperature=−18 °C, final temperature=0 °C (center), air temperature=25 °C, relative humidity=75%, h=5 W/(m² °C), external power=600 W

(m^2 °C), $k'_m = 4.081 \times 10^{-8}$ m/s, external power=600 W) as a function of thawing times at different sections of the cube height. A marked increase in the temperature can be observed in the thawed zone leading to nonuniform thermal profiles. In the analyzed conditions when the center reached 0 °C (defined as thawing time), the corner attained 100 °C.

Figure 5c shows the changes in the average humidity content (0.17%) in the minced beef cube already described as a function of thawing times. Taking into account that the average humidity values did not change markedly during the thawing process, the dependency of the physical, transport, and dielectric properties with water content was not considered.

Besides, the shape of the water profiles was maintained during the whole process with an inner zone of the cube wet with a flat humidity profile, decreasing the water content mainly at the corners.

Effect of Product Size on Microwave Thawing Times in Comparison with Conventional Thawing

One of the main factors affecting thawing dynamics is product size; this effect was studied in infinite slabs (Virtanen et al. 1997) and cylinders (Zeng and Faghri 1994), however, studies in 3D heat transfer systems were not found in the literature. In the present work, the effect of size in a cube (Lx=Ly=Lz), as well as the aspect ratio for three different cases of rectangular parallelepipeds with Lx=Ly and Lz=Lx or Lz=2Lx or Lz=3Lx, were analyzed. Figure 6 shows these effects on microwave thawing times in 3D heat transfer.

The mathematical model was also solved considering Q=0 in Eq. 1 in order to compare microwave thawing times with those obtained in the conventional method maintaining the same operating conditions (initial temperature=−18 °C, final temperature=0 °C [center], air temperature=25 °C, relative humidity=75%, h=5 W/(m² °C), external power=600 W). As can be observed, thawing times are significantly reduced using microwaves. For example, a cube of 15 cm size shows a microwave thawing time of 78 min, while the conventional thawing time was 1,263 min. However, it must be taken into account that, with a continuous application of microwaves, maximum temperatures achieved at the corners are very high, leading to nonuniform thermal profiles.

Fat Layer Size in Meat–Fat Systems

The mathematical model was used to analyze the effect of a surface fat layer on temperature profiles and thawing times of meat products. The model takes into account the appropriate electromagnetic (Pace et al. 1968) and thermal properties (Houška 1997) of beef meat and fat (Table 1). In the case of fat, different equations were used to estimate density (in
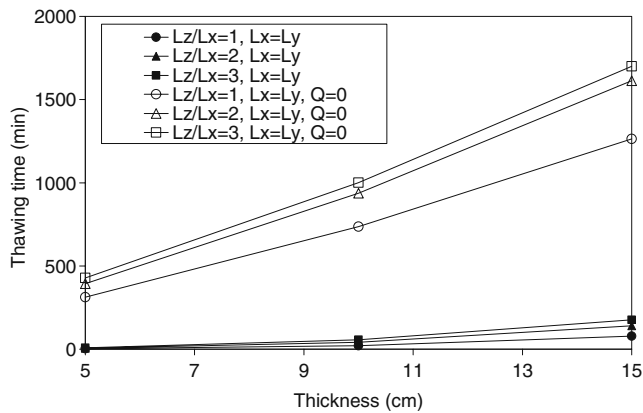
Fig. 6 Effect of meat product size and shape on microwave and conventional thawing times. Initial temperature=−18 °C, final temperature=0 °C (center), air temperature=25 °C, relative humidity=75%, h= 5 W/(m² °C), external power=600 W

kilograms per cubic meter) and thermal conductivity (in Watts per meter per degrees Celsius) at temperatures above and below 30 °C.

Figure 7a shows that the power absorbed by the meat decreased due to the presence of a fat layer with values of $f'<1$ calculated by using Eq. 20. As can be observed, increasing the thickness of the fat layer decreased the value of f' and the power absorbed by the meat.

Temperature profiles for a beef slab (meat=10 cm thickness) with two external layers of fat (5 cm thickness each one) located at both sides were simulated; one half of this system is shown in Fig. 7b. It can be observed that, when the product remains frozen, temperature profiles are uniform because the dielectric properties of the fat and the frozen product make them almost transparent to radiation. As liquid was produced during thawing, a maximum of the temperature in the thawed meat–fat interface that remained over the whole thawing process was observed. As was previously mentioned, not only ice melting was considered but also fat melting was included in this model. Gunasekaran (2002) studied the microwave heating of meat products with different fat contents, but not with a surface fat layer whose location is very important for the development of temperature profiles (Barringer et al. 1994; Rattanadecho 2004).

Simulation of the Effect of Microwave Power, Air Convection, and Combined Operation

Uniform temperature profiles are recommendable when microwave thawing is applied, taking advantage of the volumetric heat generation, to minimize weight losses and to speed up the process without producing a sharp temperature increase.

In the present work, the numerical model was applied to simulate the combination of continuous microwave power

with simultaneous application of air convection in order to attain increasing uniformity on the temperature profiles.

Figure 8a shows the effect of different power values on thawing times. For microwave thawing without air convection ($h=0$), the use of higher power levels led to marked reductions in thawing times; as an example, the reduction was 84% when the power increased from 60 to 600 W. When air convection was considered (air temperature 70 °C), thawing times decreased at low power values; however, at high power values, the heat transfer coefficient had no practical effect on thawing times. This result is in agreement with data reported by other authors (Taoukis et al. 1987; Chamchong and Datta 1999).

When external power was high (600 W), temperature profiles became nonuniform (NU=42 °C calculated with Eq. 22) with marked temperature gradients across the sample; besides, air convection at low power levels (60 W) contributed to the decrease in these nonuniform thermal distributions (NU=37 °C).

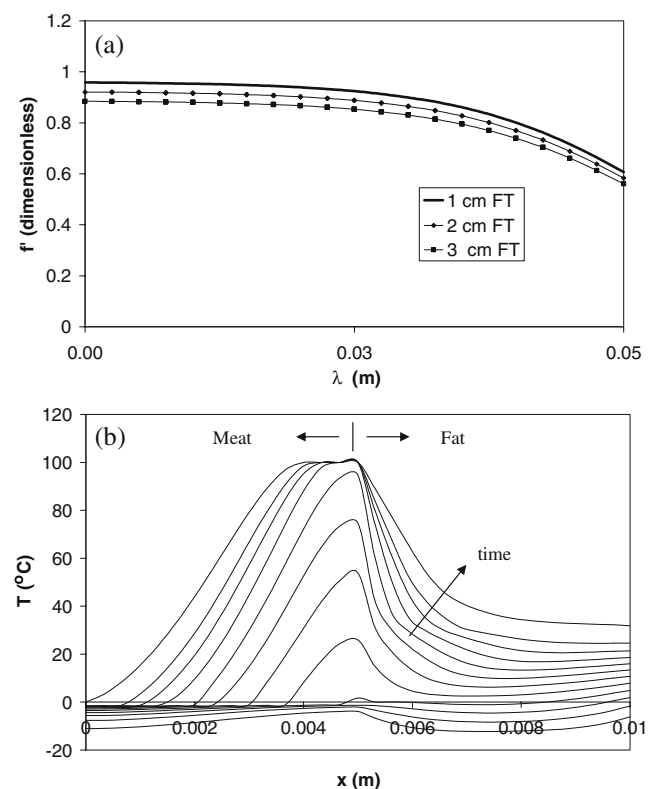The effect of air convection and microwave power values (combined thawing process) on weight losses (WL)

Fig. 7 **a** f' factor calculated by Eq. 20 that determines the decrease of the power absorbed by the meat piece as a function of the thawing front position for different values of fat layer thickness (FT). **b** Temperature profiles predicted by the mathematical model during thawing of system of a beef slab (10 cm) with a surface fat slab (5 cm). Initial temperature=−18 °C, final temperature=0 °C (center), air temperature=25 °C, relative humidity=75%, $\underline{h}$=5 W/(m² °C), external power=100 W
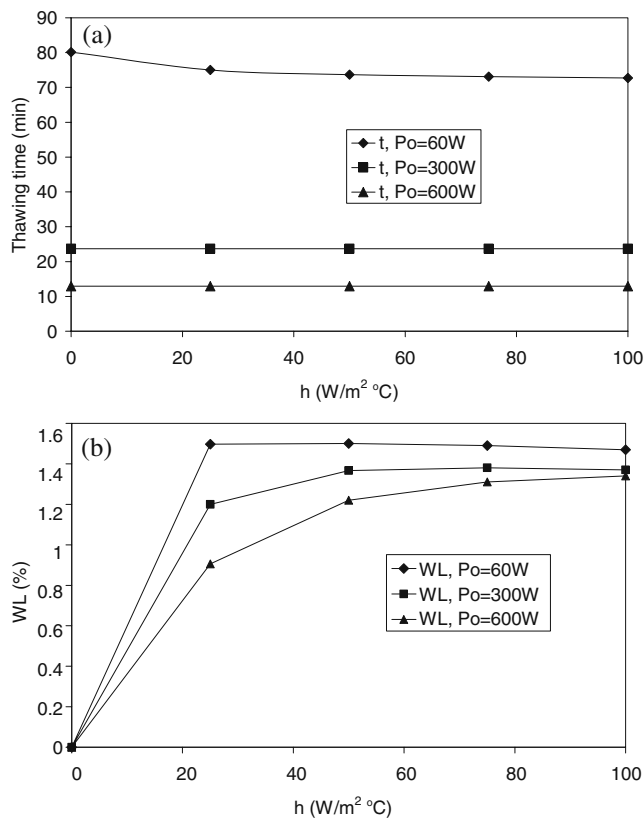
Fig. 8 Effect of power values (P_o) and heat transfer coefficient (h) on **a** thawing times and **b** weight losses. Meat slab thickness=10 cm, initial temperature=−18 °C, air temperature=70 °C

are shown in Fig. 8b; at high power levels, weight losses decreased due to the shorter thawing times. As observed, the numerical model permitted to select conditions in order to accelerate combined thawing process, maintaining acceptable dehydration levels.

Microwave Power Cycles and Refrigerated Air Convection with Controlled Surface Temperature

The use of power cycles is another strategy to decrease nonuniformities in the temperature profiles. Temperature gradients lessen when on–off power cycles are used, but this technique cannot control the hot temperature spots in the product. An interesting option is to utilize control loops that operate on the magnetron as a function of the permitted maximum temperatures located near the surface in the case of 1D heat transfer and near the corners in 3D geometries.

Refrigerated air convection (air temperature=0 °C) can be applied simultaneously with the microwave process to keep temperatures low when the magnetron is turned on and, especially, when it is off.

In the present work, this controlled thawing method was simulated; the predicted thawing times are shown in Fig. 9a (left axis). Refrigerated air convection with high h values

helped to reduce thawing times since, as product temperature is maintained low, the magnetron can remain switched on for a longer time (right axis), taking better advantages of microwave radiation thawing. Processing times became longer than those for continuous power operation; however, maximum temperatures were controlled under established values.

With reference to water transfer, foodstuff must be protected to avoid quality losses. Food products without an impermeable water vapor packaging, submitted to intermittent microwave thawing with simultaneous air convection, show an increase of the weight losses (WL; Fig. 9b) as air velocity rises. Similar results were reported by Virtanen et al. (1997) and Taher and Farid (2001).

Conclusions

In this work, coupled microscopic energy and mass balances representing microwave thawing were numerically solved. A moving front between the frozen and unfrozen
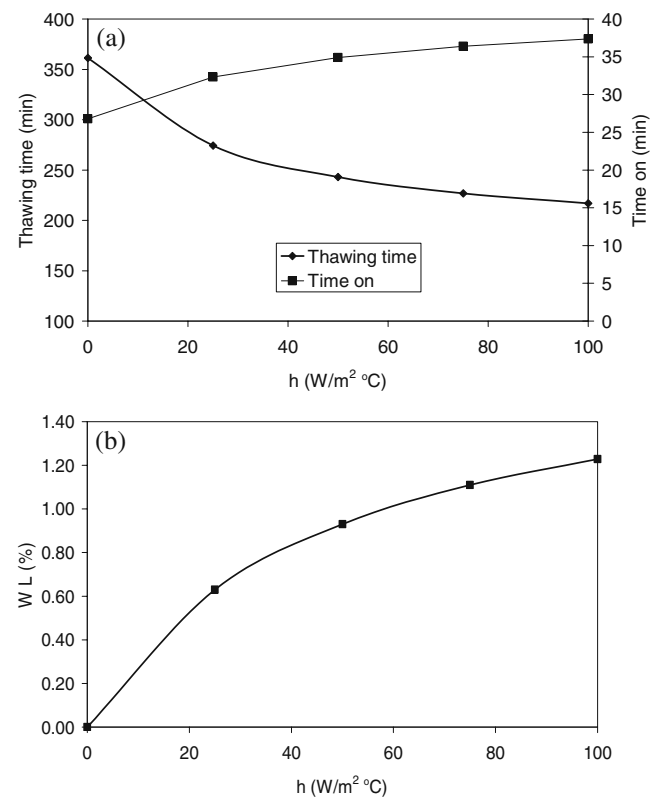

Fig. 9 Effect of refrigerated air convection (h values) with simultaneous operation of microwave power cycles on **a** thawing times (*left axis*) and the time that the magnetron is switched on to reach the maximum allowed temperature (10 °C) on the surface of a meat slab (*right axis*) and **b** weight losses. Meat slab size=10 cm, initial temperature= −18 °C, maximum temperature allowed on surface=10 °C, air temperature=0 °C, external power=100 W

zones was considered; the model can be applied to simulate the behavior of large systems for which Lambert's law is valid. The absorbed power at the surface was considered depending on the characteristics of the product; it was determined for water and corrected for the case of unfrozen, partially frozen, or totally frozen product.

The heat and mass transfer model was compared with results reported in the literature in one and two dimensions. The 3D model agreed with the experimental thermal histories measured at the center and the corners of frozen meat cubes thawed in our laboratory microwave equipment.

The model was assessed to predict temperature, water concentration profiles, and thawing times in meat products. The simulated thawing times were lower for the microwave process in comparison with the conventional method (using air at 25 °C) for different meat product sizes.

In meat systems with a surface fat layer, a distortion of the temperature profiles evidenced by the presence of maximum temperatures at the fat–thawed product interface was determined by the numerical model.

The model was also run to analyze the combined effect of air convection and microwave power cycles on thawing times. In continuous operation, the use of hot air convection helped to decrease nonuniformities in the temperature profiles, especially at low power levels. When operating with power cycles, the use of refrigerated air convection contributed to decrease the product temperature so the magnetron keeps switched on, for longer times, getting a more effective use of the microwave radiation for thawing.

References

Ahmed, J., & Ramaswamy, H. S. (2007). Microwave pasteurization and sterilization of foods. In M. S. Rahman (Ed.), *Handbook of food preservation* (2nd ed., pp. 691–711). USA: CRC.

Ayappa, K. G. (1997). Modelling transport processes during microwave heating: A review. *Reviews in Chemical Engineering, 13*(2), 1–67.

Ayappa, K. G., Davis, H. T., Crapiste, G., Davis, E. A., & Gordon, J. (1991). Microwave heating: An evaluation of power formulations. *Chemical Engineering Science, 46*(4), 1005–1016.

Barringer, S. A., Davis, E. A., Gordon, J., Ayappa, K. G., & Davis, H. T. (1994). Effect of sample size on the microwave heating rate: Oil vs water. *American Institute of Chemical Engineering Journal, 40*, 1433–1439.

Basak, T., & Ayappa, K. G. (2002). Role of length scales on microwave thawing dynamics in 2D cylinders. *International Journal of Heat and Mass Transfer, 45*, 4543–4559.

Bird, R. B., Stewart, W. E., & Lightfoot, E. N. (1976). *Transport phenomena*. New York: Wiley.

Burfoot, D., Railton, C. J., Foster, A. M., & Reavell, S. R. (1996). Modelling the pasteurisation of prepared meals with microwaves at 896 MHz. *Journal of Food Engineering, 30*, 117–133.

Campañone, L. A. (2001). *Transferencia de calor y materia en congelación y almacenamiento de alimentos, sublimación de hielo, calidad, optimización de condiciones de proceso*. Ph.D. Thesis, Facultad de Ingenieria, Universidad Nacional de La Plata, Argentina.

Campañone, L. A., & Zaritzky, N. E. (2005). Mathematical analysis of microwave heating process. *Journal of Food Engineering, 69*, 359–368.

Chamchong, M., & Datta, A. K. (1999). Thawing of foods in a microwave oven: I. Effect of power levels and power cycling. *Journal of Microwave Power and Electromagnetic Energy, 34*(1), 9–21.

Cha-um, W., Rattanadecho, P., & Pakdee, W. (2009). Experimental and numerical analysis of microwave heating of water and oil using a rectangular wave guide: Influence of sample sizes, positions, and microwave power. *Food Bioprocess Technology*. doi:10.1007/s11947-009-0187.

Cleland, D. J., & Cleland, A. C. (1991). *An alternating direction, implicit finite difference scheme for heat conduction with phase change in finite cylinders*. In: Proceedings of the XVIII International Congress of Refrigeration, Montreal, 356 pp.

Cleland, A. C., & Earle, R. L. (1979). Prediction of freezing times for foods in rectangular packages. *Journal of Food Science, 44*, 964–970.

Curet, S., Rouaud, O., & Boillereaux, L. (2007). Microwave tempering and heating in a single-mode cavity: Numerical and experimental investigations. *Chemical Engineering and Processing, 47*, 9–10.

Datta, A. K., & Anantheswaran, R. C. (2001). *Handbook of microwave technology for food applications*. USA: Marcel Dekker.

Geedipalli, S. S. R., Rakesh, V., & Datta, A. K. (2007). Modeling the heating uniformity contributed by a rotating turntable in microwave ovens. *Journal of Food Engineering, 82*, 359–368.

Gunasekaran, N. (2002). *Effect of fat content and food type on heat transfer during microwave heating*. M.S. Thesis, Virginia Polytechnic Institute and State University, Virginia, USA.

Gunasekaran, S., & Yang, H. (2007). Effect of experimental parameters on temperature distribution during continuous and pulsed microwave heating. *Journal of Food Engineering, 78*(4), 1452–1456.

Hui, Y. H. (2006). *Handbook of food science, technology and engineering*. USA: CRC.

Houška, M. (1997). *Meat, meat products and semiproducts. Thermophysical and rheological properties of foods*. Prague: Food Research Institute Prague.

Jeong, J. Y., Lee, S. E., Choi, J. H., Lee, J. Y., Kim, J. M., Min, S. G., et al. (2007). Variability in temperature distribution and cooking properties of ground pork patties containing different fat level and with/without salt cooked by microwave energy. *Meat Science, 75*(3), 415–422.

Lee, M. Z. C., & Marchant, T. R. (1999). Microwave thawing of slabs. *Applied Mathematical Modelling, 23*, 363–383.

Lin, Y. E., Anantheswaran, R. C., & Puri, V. M. (1995). Finite element analysis of microwave heating of solid foods. *Journal of Food Engineering, 25*, 85–112.

Lin, T. M., Durance, T. D., & Scaman, C. H. (1998). Characterization of vacuum microwave, air and freeze dried carrot slices. *Food Research International, 31*(2), 111–117.

Liu, C. M., Wang, Q. Z., & Sakai, N. (2005). Power and temperature distribution during microwave thawing, simulated by using Maxwell's equations and Lambert's law. *International Journal of Food Science and Technology, 40*, 9–21.

Mudgett, R. E. (1982). Electrical properties of foods in microwave processing. *Food Technology, 36*, 109–115.

Ni, H., & Datta, A. K. (2002). Moisture as related to heating uniformity in microwave processing of solids foods. *Journal of Food Process Engineering, 22*, 367–382.

Oliveira, M. E. C., & Franca, A. S. (2002). Microwave heating of foodstuffs. *Journal of Food Engineering, 53*, 347–359.

Pace, W. E., Wetsphal, W. B., & Goldblith, S. A. (1968). Dielectric properties of commercial cooking oils. *Journal of Food Science, 33*, 30–33.

Pangrle, B. J., Ayappa, K. G., Davis, H. T., Davis, E. A., & Gordon, J. (1991). Microwave thawing of cylinders. *AIChE Journal, 37*(12), 1789–1800.

Rattanadecho, P. (2004). Theoretical and experimental investigation of microwave thawing of frozen layer using a microwave oven (effects of layered configurations and layer thickness). *International Journal of Heat and Mass Transfer, 47*, 937–945.

Sakiyan, O., Sumnu, G., Sahin, S., Meda, V., Koksel, H., & Chang, P. (2009). A study on degree of starch gelatinization in cakes baked in three different ovens. *Food Bioprocess Technology.* doi:10.1007/s11947-009-0210-2.

Sanz, P. D., Dominguez, M., & Mascheroni, R. H. (1987). Thermophysical properties of meat products. General bibliography and experimental data. *Transactions of the ASAE, 30*, 283.

Taher, B. H., & Farid, M. M. (2001). Cyclic microwave thawing of frozen meat: Experimental and theoretical investigation. *Chemical Engineering and Processing, 40*(4), 379–389.

Taoukis, P., Davis, E. A., Davis, H. T., Gordon, J., & Talmon, Y. (1987). Mathematical modeling of microwave thawing by the modified isotherm migration method. *Journal of Food Science, 2*, 455–463.

Tong, C. H., & Lund, D. B. (1993). Microwave heating of baked dough products with simultaneous heat and moisture transfer. *Journal of Food Engineering, 19*, 319–339.

Turabi, E., Sumnu, G., & Sahin, S. (2008). Optimization of baking of rice cakes in infrared–microwave combination oven by response surface methodology. *Food Bioprocess Technology, 1*, 64–73.

Vadivambal, R., & Jayas, D. S. (2009). Non-uniform temperature distribution during microwave heating of food materials—A review. *Food Bioprocess Technology.* doi:10.1007/s11947-008-0136-0.

Virtanen, A. J., Goedeken, D. L., & Tong, C. H. (1997). Microwave assisted thawing of model foods using feedback temperature control and surface cooling. *Journal of Food Science, 62*(19), 150–154.

Zeng, X., & Faghri, A. (1994). Experimental and numerical study of microwave thawing heat transfer for food materials. *Transactions of ASME, 116*, 446–455.